Title	Temporal and Spatial Variations of Monthly Rainfall in Java, Indonesia
Author(s)	Yasunari, Tetsuzo
Citation	東南アジア研究 (1981), 19(2): 170-186
Issue Date	1981-09
URL	http://hdl.handle.net/2433/56055
Right	
Type	Journal Article
Textversion	publisher

Southeast Asian Studies, Vol. 19, No. 2, September 1981

Temporal and Spatial Variations of Monthly Rainfall in Java, Indonesia

Tetsuzo YASUNARI*

Abstract

The analysis of the long-term fluctuation of monthly rainfall (1951–1973) revealed that the year-to-year variability of the rainfall in and around Java is large in the "east monsoon" (dry) season and relatively small in the "west monsoon" (rainy) season. The empirical orthogonal function analysis of the anomaly rainfall showed that the quasi-biennial oscillation (QBO) is dominant over the whole of Java with the large variance (29.4% of the total variance), and that a large variability in the "east monsoon" season is mostly explained by this component. The second component (6.2% of the total variance) represents the variation in the "west monsoon" season with a contrastive spatial pattern between the Java Sea side and the Indian Ocean side of the island. It was also confirmed that the first component (the QBO mode) in the anomaly rainfall is closely connected with the QBO in the surface pressure field over Australasia through the eastern south Pacific and the second component is associated with the north- (or south-) ward shift of the winter monsoon circulation system in the Northern Hemisphere. In addition, the relations between these two modes and the "southern oscillation" are briefly discussed.

I Introduction

The broad area of the Indonesian islands including New Guinea is called the tropical "maritime continent," and is described as one of the most humid areas in the world. The annual rainfall amount exceeds 3,000 mm in a large part of this area, and in mountainous and hilly places of some islands it is not uncommon to find the annual amount over 4,000 mm. The vast release of latent heat through cummulus convection and rainfall contributes in forming one of the greatest heat sources of the global atmosphere, which in turn may have a great role in the atmospheric circulations. For example, it has been pointed out that the year-to-year variation of the intensity of this heat source largely affects the strength of the subtropical jet stream over far-east Asia [Ramage 1968]. On the other hand, this area is also known as one of the centers of action for large-scale atmospheric circulations in the Southern Hemisphere called the "southern oscillation," which was discovered by Walker (Walker [1924], Walker and Bliss [1932; 1937], etc.). This circulation represents the standing oscillation in the pressure field between the eastern Pacific and Australia through the Indian

* 安成哲三, The Center for Southeast Asian Studies, Kyoto University

Ocean with a time scale of two to ten years or so. In recent years, it has been found that this oscillation consists of the zonally oriented circulation cell along the equatorial Pacific region [Bjerknes 1969]. In a mean state, the upward motion is located over the warm and moist "maritime continent" and the downward motion is located over the cool and dry eastern Pacific. In other words, it seems that this oscillation derives its propulsion from the longitudinal heating contrast and its variability. In this context, the rainfall variations of the Indonesian region should be noted as one of the key factors in understanding the physical process of the atmospheric circulations in the tropics.

However, detailed analysis of the temporal and spatial variations of the rainfall over this region have not been undertaken, mostly because of a lack of available data. Tanaka [1980] scrutinized the fluctuation of the monsoon circulations over south, southeast and east Asia and associated general circulation patterns for both northern winter and summer monsoon. He also paid great attention to the southern oscillation as an important factor in controlling monsoon activity. However, his analysis of the variation of rainfall especially for the Indonesian region was not sufficient, because observation points utilized over there were sparse. Very recently, Kamimoto [1981] studied the secular variations of the summer monsoon rainfall over the whole and regional areas of monsoon Asia, by using the empirical orthogonal function analysis. One of his conclusions was that the dominant mode in the Indonesia-Malaysia region (36 stations) is closely related to the southern oscillation. Unfortunately, since his analysis was based on data for the northern summer monsoon months (June to August), he did not discuss the exact time scales and seasonal dependencies of the dominant modes.

In this paper, we attempt to reveal the time-space characteristics of the seasonal and non-seasonal variations of rainfall in Java island, where data is available from a relatively large number of stations in comparison with the other islands. The atmospheric circulation patterns associated with the extracted dominant rainfall patterns will also be examined.

II Data

Monthly rainfall data from 54 stations in Java and the surrounding small islands (Madura, Bali and Lombok) was the fundamental data source for the present analysis. In addition, data from 29 stations in Sumatra, Borneo and Sulawesi were used. The time period of the data set was 23 years from 1951 to 1973, though two years' data for 1954 and 1955 were missing from all the stations. The data source was "Pemeriksaan Hudjan Di Indonesia (Rainfall Observations in Indonesia)" published by the Institute of Meteorology and Geophysics, Department of Communications, Indonesia. The locations of the stations in and around Java are shown in Fig. 1, and the names, the mean

Table 1 List of the Names, the Mean Monthly and Annual Rainfall of the Stations in and around Java

St.	Name	Jan.	Feb.	Mar.	Apr.	May	Jun.	Jul.	Aug.	Sept.	Oct.	Nov.	Dec.	Annual Total
1	Menes	532	429	492	345	269	196	164	141	166	260	449	591	4034
2	Jasinga	344	278	349	347	270	194	159	167	194	270	230	258	3060
3	Jakarta	370	303	250	123	117	93	55	54	57	85	121	172	1800
4	Jatisari	376	342	271	171	150	77	65	39	33	88	204	292	2108
5	Pondokbales	451	461	455	432	286	152	153	105	106	220	319	384	3524
6	Cikencreng	206	192	260	311	317	381	484	271	304	467	512	317	4022
7	Plabuhan Ratu	318	280	278	198	146	99	87	63	64	138	283	336	2290
8	Cempaka	293	271	355	339	304	148	120	136	175	258	297	324	3020
9	Ciranjang	232	205	238	228	163	69	101	99	89	147	186	235	1992
10	Paseh	311	249	330	256	181	82	93	58	78	124	223	326	2311
11	Darmaradja	421	307	433	290	180	92	83	33	38	106	235	429	2647
12	Anjatan	433	288	219	106	95	59	57	32	15	49	116	205	1674
13	Ciawigebang	374	297	324	210	202	86	71	47	32	88	211	327	2269
14	Kubangwaru	359	275	264	166	116	75	54	41	27	66	159	275	1877
15	Bumiay	399	344	405	265	185	119	73	60	42	139	202	354	2587
16	Bantarbolang	656	513	440	266	249	134	106	71	70	101	228	413	3247
17	Bandarsiday	921	689	606	425	317	147	170	134	143	180	333	548	4613
18	Lumbir	344	338	368	245	227	130	120	92	72	194	307	341	2778
19	Maos	228	187	276	162	185	151	158	65	85	203	291	254	2245
20	Wanadadi	462	393	497	401	286	180	122	81	71	237	469	486	3685
21	Kedungsamak	398	354	403	265	229	129	72	68	58	235	441	473	3125
22	Bener	487	489	414	269	209	117	78	54	38	117	343	472	3087
23	Badran	300	332	332	231	166	94	77	49	61	87	199	303	2231
24	Wijilan	333	312	289	160	120	55	59	23	17	79	188	258	1893
25	Colomadu	306	319	308	243	141	60	62	33	33	118	193	285	2101
26	Baturetno	369	326	327	167	111	53	34	21	16	77	125	292	1918
27	Mojo Sragen	291	313	334	207	133	60	59	25	37	124	229	263	2075
28	Puguh	480	297	230	177	130	86	88	52	46	84	170	247	2087
29	Karang	431	355	420	331	243	126	107	73	74	149	276	420	3005
30	Cluwak	904	610	437	225	220	168	106	93	59	63	159	424	3468
31	Tawangharjo	306	256	230	110	77	67	69	50	71	122	207	280	1845
32	Rembang	205	158	212	86	99	49	30	20	16	30	120	198	1223
33	Randublatung	251	233	278	144	138	72	52	38	55	140	229	291	1921
34	Jenu	239	134	159	139	109	57	60	18	23	43	117	188	1286
35	Ngimbang	295	289	347	206	151	56	33	27	28	74	238	293	2037
36	Mojokerto	363	365	325	169	123	40	31	7	7	47	109	295	1881
37	Kendal	351	443	404	307	218	80	66	40	24	123	220	379	2655
38	Lembean	286	275	293	202	152	53	43	16	10	50	153	286	1819
39	Pacitan	356	334	294	99	126	77	87	42	68	148	228	324	2183
40	Widoro	261	233	230	173	162	62	76	21	62	99	144	214	1737
41	Kaliputih	309	237	268	231	154	83	67	30	28	113	197	408	2125
42	Randupitu	384	346	356	195	174	56	24	9	0	24	92	294	1954
43	Pasirian	208	217	240	151	151	90	94	37	60	130	189	246	1813
44	Jatiampoh	326	307	280	98	86	18	41	13	9	20	63	205	1466
45	Bungatan	369	376	244	70	46	21	26	8	4	13	49	161	1387
46	Tempuran	392	305	373	213	134	62	57	25	38	95	195	347	2236
47	Lewung	230	204	194	93	71	28	10	12	4	17	61	189	1113
48	Kraden	213	238	226	91	97	78	70	25	24	61	89	197	1409
49	Konang	266	191	268	167	134	63	56	20	24	72	140	225	1626
50	Tlanakan	177	184	179	129	117	48	36	11	5	31	83	196	1196
51	Batang-Batang	280	184	197	151	104	62	50	13	8	36	109	228	1422
52	Grogak	301	283	220	111	83	30	37	20	5	24	49	159	1322
53	Tianyar	232	234	203	70	43	20	34	5	0	8	34	141	1024
54	Ampenan	247	210	120	80	74	45	42	28	23	90	117	224	1300
	Areal Mean	355	307	310	204	162	91	82	52	54	114	202	301	2235

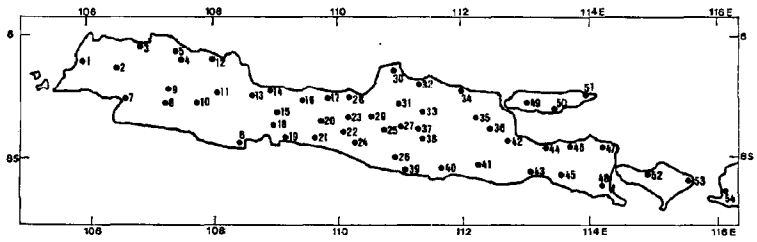

Fig. 1 Locations of the stations in Java, Madura, Lombok and Bali islands. Station numbers in Table 1 are also indicated.

monthly and the annual rainfall amounts of the 54 stations are summarized in Table 1.

III Seasonal Variation and Its Variability

It is well known that the seasonal variation of rainfall show a distinct annual cycle with the maximum in the months from December to March and the minimum in the months from June to September in most parts of Java. The rainy season corresponds with the northeast monsoon period in the northern winter, and the dry season with the southwest monsoon period in the northern summer. The prevailing wind over this area is W to WNW in the rainy season, and E to ESE in the dry season. Therefore, the local people in Java call the rainy season "*angin barat* (west monsoon)" and the dry season "*angin timur* (east monsoon)." The mean rainfall distributions for the rainy season (Dec. to Mar.) and the dry season (Jun. to Sept.) are shown in Fig. 2.

It should be noted, however, that the "rainy" and the "dry" seasons deduced as climatological mean values are not as stable as those in the continental monsoon regions of India and Southeast Asia. For example, Fig. 3 shows the series of monthly rainfall and the normal-year values at Lumbir in central Java, where the mean annual rainfall is nearly 2,800 mm (refer to Table 1). A large variation from month to month is apparent in this figure. Typically in 1957, July rainfall reached more than 700 mm but rainfall amount in "rainy" months were relatively small, while in 1972 no rainfall occurred in the "dry" months. To estimate the variability of the anomalies from the

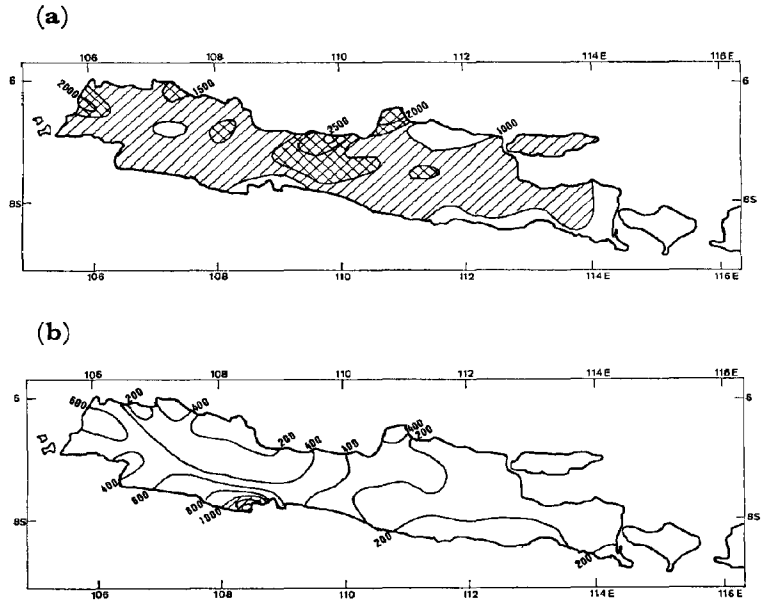

Fig. 2 Distributions of the rainfall amount for (a) the rainy season (December to March), and (b) the dry season (June to September). The areas of the rainfall amount over 1,000 mm are shaded in both figures, and the areas over 1,500 mm are cross-hatched in (a).

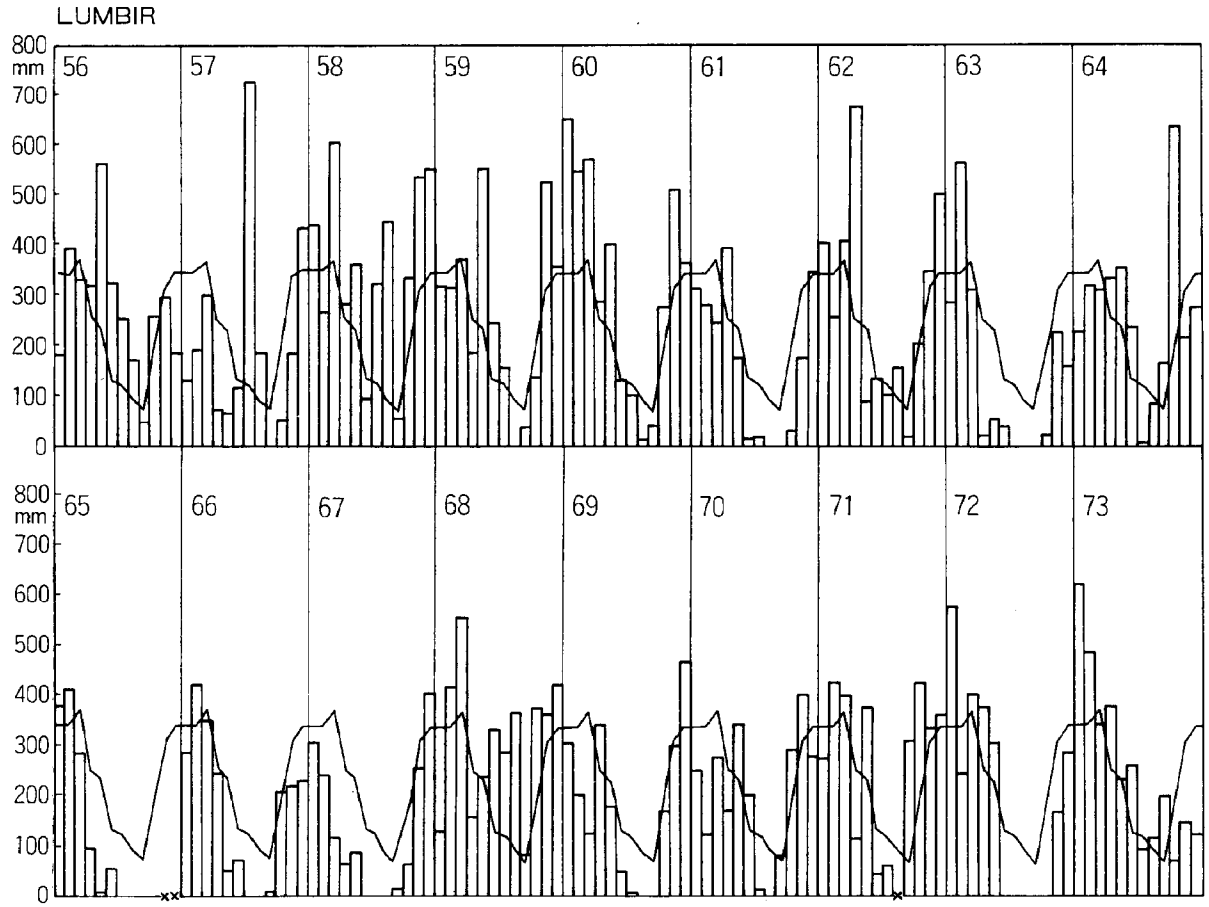

Fig. 3 Series of monthly rainfall at Lumbir, central Java. The normal monthly values are also shown with solid lines.

normal (or climatological mean) values, the variance of the anomalies (V_a) and its ratio to the total variance (V_t) were calculated for each station. That is:

$$R(i)=\frac{V_a(i)}{V_t(i)}=\frac{\sum_t(P(i,t)-P_n(i,t))^2}{\sum_t(P(i,t)-\overline{P(i,t)})^2}$$

where $P(i,t)$ is the monthly rainfall, $P_n(i,t)$ is the normal monthly rainfall, and $\overline{P(i,t)}$ is the long-term mean rainfall for the whole period (1951–1973) for the i-th station. Here, $P_n(i,t)$ was defined as the averaged values of the 23 years' data for each month.

The spatial distribution of $R(i)$ is shown in Fig. 4. As the total variance $V_t(i)$ may roughly be the sum of $V_a(i)$ and the variance of the mean seasonal variation (i.e., the variance of $P_n(i,t)$), the area of $R(i)$ ($\geqq 0.5$) may correspond with the area where the month-to-month anomaly

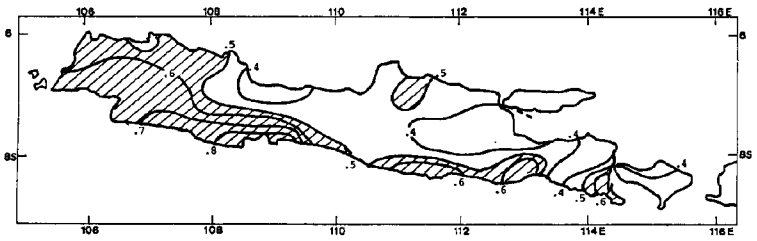

Fig. 4 Spatial distribution of $R(i)$ (the ratio of V_a to V_t). The areas of the values ($\geqq 0.5$) are shaded.

variation is larger in amplitude than the mean seasonal variation. In the whole area the ratio exceeds 0.3. Interestingly, the area of large values is mainly on the Indian Ocean side, where the rainfall during the "east monsoon" is relatively large (as referred to in Fig. 2). Thus, the large variability of the anomaly rainfall in Java may be mostly attributed to the fluctuation of the "east monsoon" which may be closely related to the atmospheric circulations in the southern winter.

IV Dominant Patterns of the Anomaly Rainfall in Time-space Field

IV-1. Empirical Orthogonal Function (EOF) Analysis

The above results suggested that the month-to-month or year-to-year deviations from the normal values have relatively large amplitudes even compared to the mean seasonal variations. The empirical orthogonal function (EOF) analysis was adopted to deduce some dominant spatial patterns and their temporal variations of the anomaly rainfall. To avoid the missing data for 1954 and 1955, the data for 18 years from 1956 to 1973 was used. Before applying EOF analysis, the anomaly rainfall values were normalized by dividing them by the standard deviation:

$$P'(i, t)=(P(i, t)-P_n(i, t))/\sqrt{V_a(i)}$$

Then, the normalized anomaly rainfall $P'(i, t)$ was expanded to the EOFs as follows:

$$P'(i, t)=\sum_{m=1}^{N} F_m(i)f_m(t) \qquad (1)$$

where $F_m(i)$ is the space coefficient of the i-th station and $f_m(t)$ is the time coefficient of the time t for the m-th component. Equation (1) was obtained under the condition of orthogonarity of time functions for an arbitrary pair of components:

$$\sum_t f_i(t)f_j(t)\begin{cases}=\lambda_i & (i=j)\\ =0 & (i\neq j)\end{cases} \qquad (2)$$

where λ_i corresponds with the variance of $f_i(t)$, which is equal to the i-th largest eigenvalue for the correlation matrix of $P'(i, t)$. The mathematical procedure to obtain equation (1) is described in the Appendix.

The variances (explained by the eigenvalues) and the cumulative fractions of the variances by the first eight components are given in Table 2. The spatial patterns (e.g., the distributions of the space coefficients), and their time coefficients for the first four components are shown, respectively, in Fig. 5 and Fig. 6.

It is conspicuous in Table 2 that the variance is concentrated to the first component (29.4%)

Table 2 Variances and Cumulative Percentage Fraction of Variances of the First Eight Components of the Anomaly Rainfall

Component	1	2	3	4	5	6	7	8
Variance (%)	29.4	6.2	5.3	4.1	3.4	3.1	3.0	2.7
Cumulative(%)	29.4	35.6	40.9	45.0	48.4	51.5	54.5	57.2

and the contributions of the other components are very small. The cumulative fraction by the first eight components occupies at most 60% of the total variance. This suggests that the rainfall in this area is greatly affected by the complex effect of local topography and variable nature of some meteorological elements even on a monthly basis. Especially, the large variability of the winds in the equatorial zone may contribute significantly to this capricious rainfall. Nevertheless, at least the first four components may be worth of attention on account of the systematic spatial patterns shown in Fig. 5 (From the fifth component the space coefficients show, more or less, random distributions.).

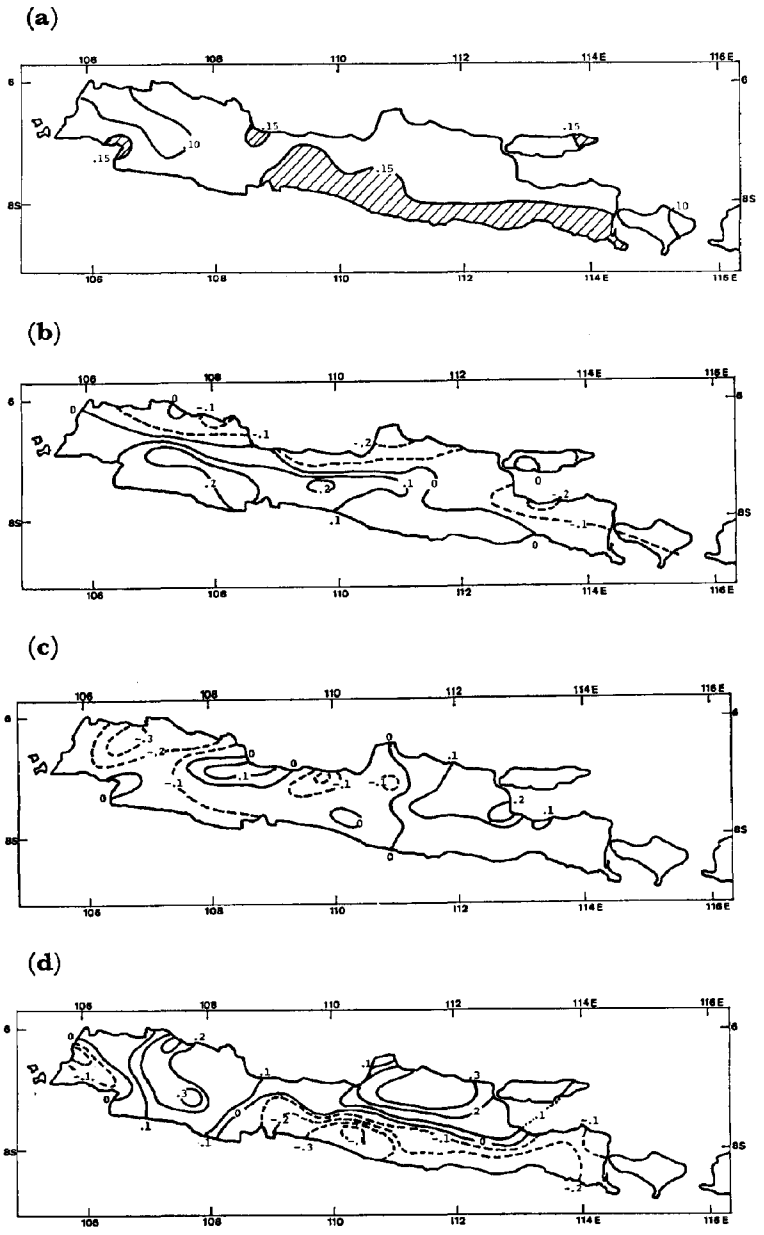

Fig. 5 Distributions of spatial coefficients of (a) the first, (b) the second, (c) the third, and (d) the fourth component. In (a), the areas larger than 0.15 are shaded.

The first component dominantly affects the whole of Java with the same sign of the space coefficients in the whole area. This implies that this mode shows nearly in-phase temporal variation in this area. The center of variation is found on the Indian Ocean side of east and central Java, and the variance is relatively small in west Java. Moreover, the EOF analysis with the addition of data from the stations in Sumatra, Borneo and Sulawesi suggested that this mode dominants a broad area of the Indonesian islands including at least the southern half of these three large islands, as shown in Fig. 7. This pattern seems to oscillate with a periodicity of about two years as shown in Fig. 5. It also seems that the time coefficients in most of the years show larger amplitudes in the dry months (May to Oct.) than in the rainy months (Nov. to

Apr.). That is, the first component may be an important factor for the variation of the "east monsoon" rainfall. This will be discussed further later.

The second component clearly expresses the contrast between the Java Sea side and the Indian Ocean side, or preferably, the contrast between the plain area of the Java Sea side and the mountainous area to the south of it, since the line of the zero value corresponds well with the border area between the plain and the mountainous region. In contrast to the first component, the large amplitudes of the time coefficients appear mostly in the rainy months from December to March, which implies that this pattern mainly represents the variation of the "west monsoon" rainfall.

The third component shows a contrastive spatial pattern between east and west Java, but its association with the topography of the island is not clear. The fourth component shows a con-

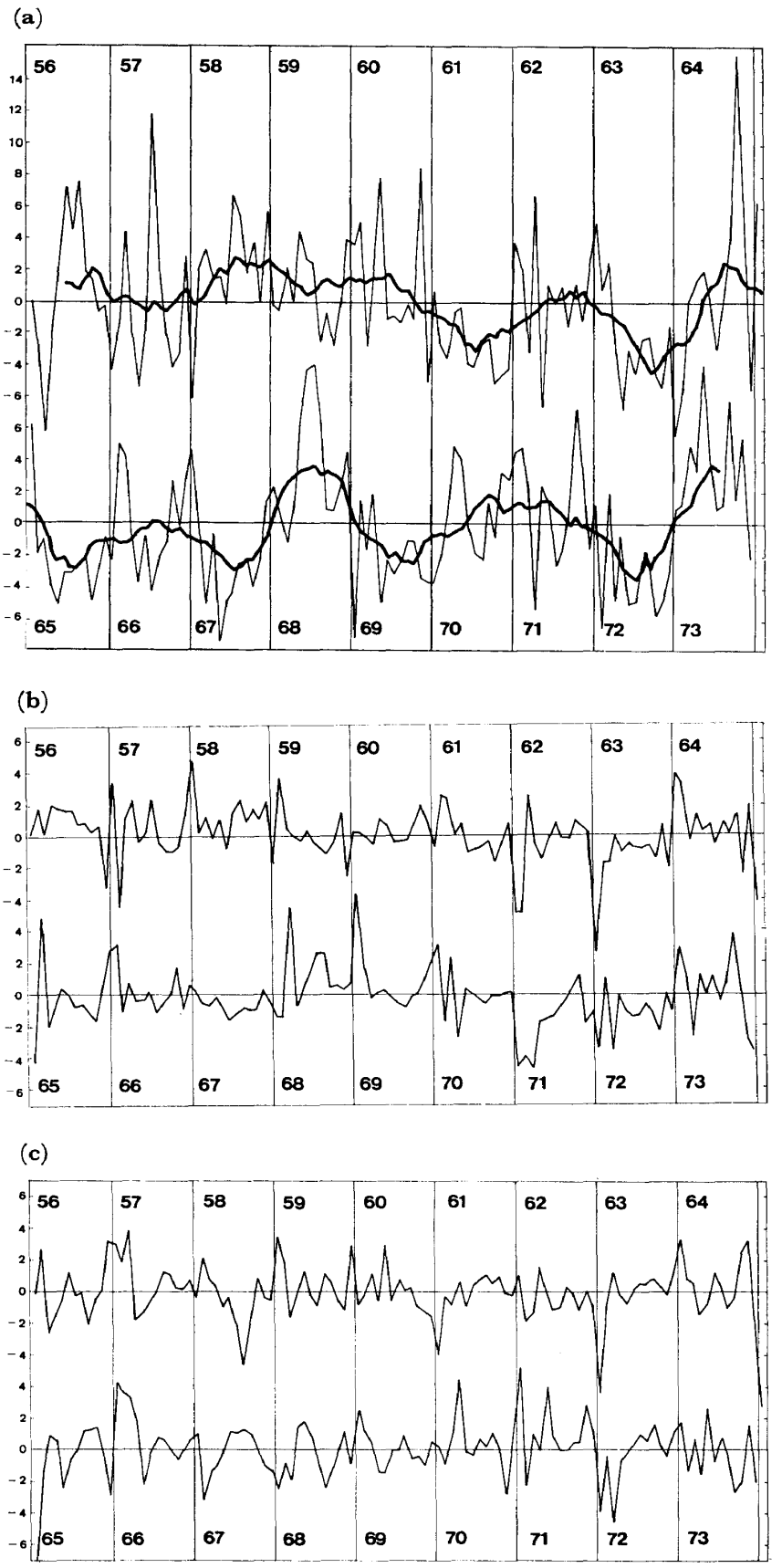

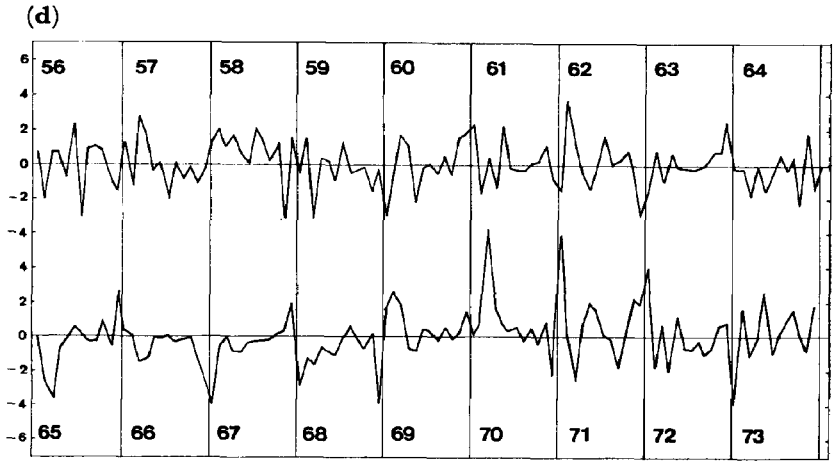

Fig. 6 Series of time coefficients of (a) the first, (b) the second, (c) the third, and (d) the fourth component. In (a) the smoothed series with 11-month running mean are also shown with solid lines.

trast between northwest and southeast Java, but it is also difficult to explain this pattern from the topography. However, as the large amplitudes of the time coefficients of these two components mostly appear in the rainy season (i.e., "west monsoon" season), it is plausible that these two spatial patterns express the windward or leeward areas associated with minor fluctuations of the prevailing winds in the rainy season.

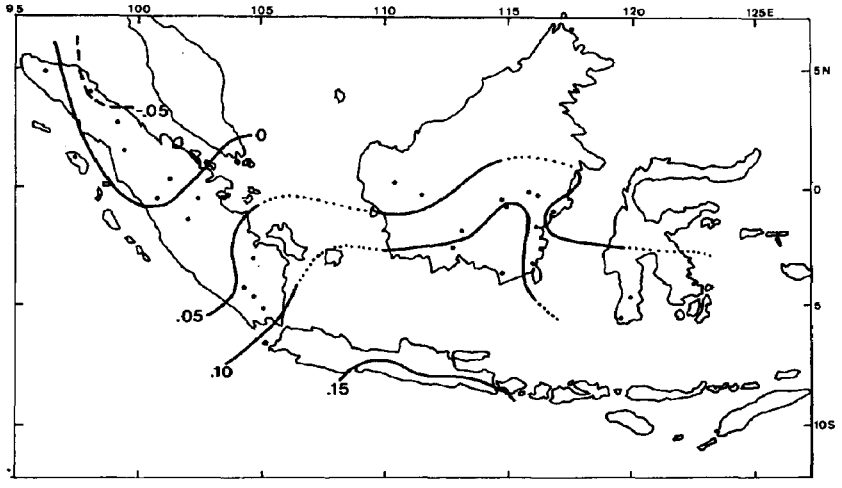

Fig. 7 Distributions of spatial coefficients of the first component over the Indonesian islands. Locations of stations excluding Java are indicated.

IV-2. Spectral Analysis

To confirm the dominant time-scales (or the periodicities) of each component, the spectral analysis was applied to the time coefficients. The lag-correlation method [Blackman and Tukey 1958] was used to obtain power spectra. The total record length was 216 days, and the maximum lag of 36 days was adopted. The results for the first four components are shown in Fig. 8.

The first component exhibited remarkably a dominant periodicity of about two years with a significant level of 95% or more. This component, therefore, may represent the quasi-biennial oscillation (QBO) in the anomaly rainfall in the Indonesian region, which may be closely connected with the QBO mode in the southern oscillation [Berlage 1961] or the QBO in the Southern Hemisphere mid-latitudes [Trenberth 1975].

The second component showed no significant peaks in the defined period range (The spectral peak of about two months may be out of resolution with the sampling interval of one month.). However, this component

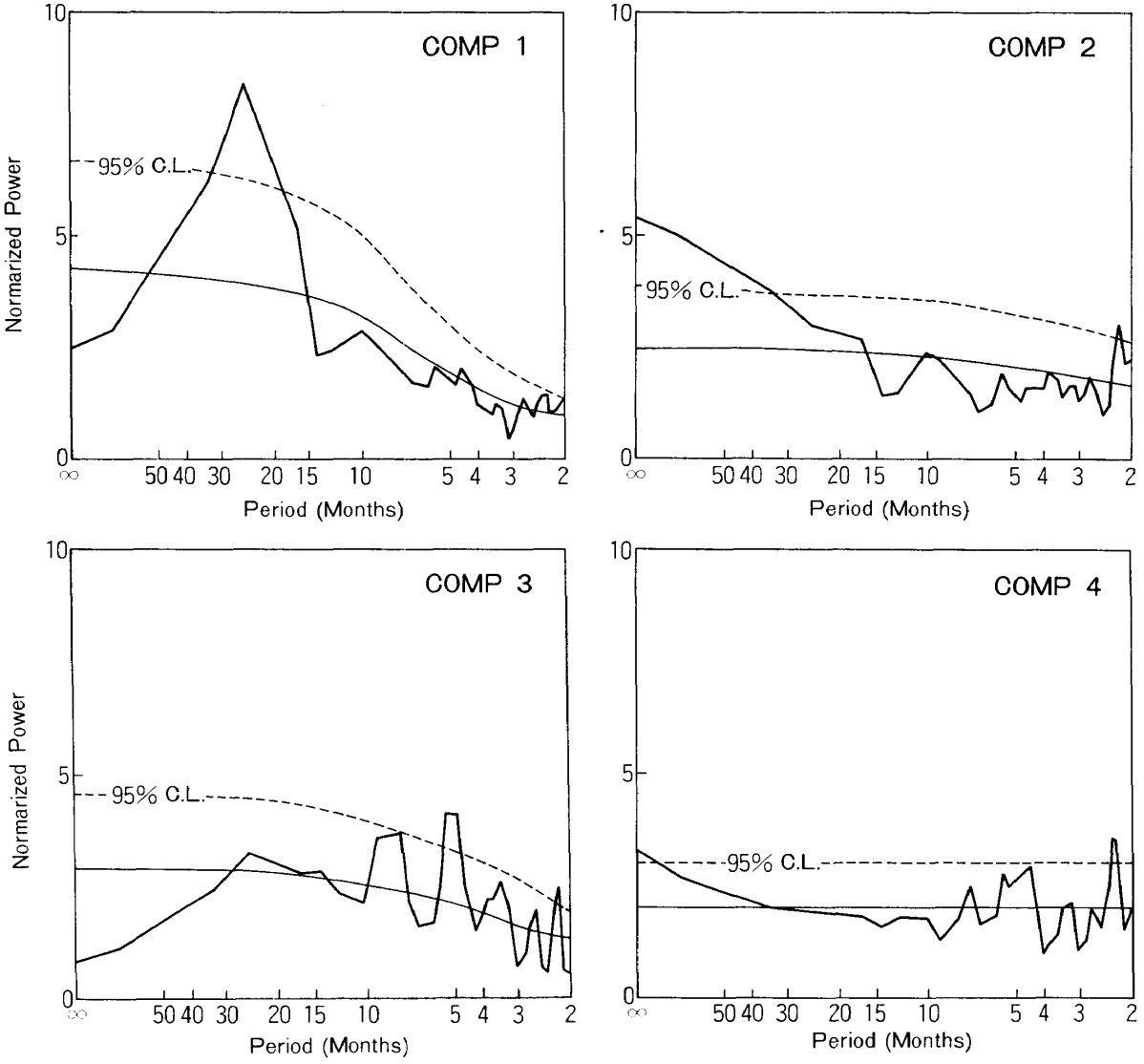

Fig. 8 Power spectra of the time coefficients for the first to the fourth component. Power spectrum is normalized by deviding them by the variance of each component. The red noise or white noise level (thin solid line), and the limit of the 95% confidence level (dashed line) are also shown in each case.

seems to have a time scale longer than three or four years if the large power densities in the low frequency range are considered. It is certain that in the original time series (Fig. 6(b)) large positive (or negative) values tended to occur in the time intervals of several years or more.

The third and fourth components showed some spectral peaks in a period range of less than 10 months. However, since these peaks are not distinguished significantly from the "white noise" level, it may be assumed that these two modes are close to a random process in the time series.

IV-3. Seasonal Dependencies

As briefly mentioned in the previous

sub-sections, some dominant patterns, especially of the first and second components, show large seasonal dependencies. This implies that the predominant contribution of the first component to the total variance in the mean may not be true for each month or season. The contributions of the first four components were estimated for each month of the year by taking the mean square of the time coefficients, as shown in Table 3. In the "east monsoon" (or dry) season the first component plays a main role in the anomaly rainfall variation while contributions of the other components are negligible. In most of the months of this season, more than a half of the total variance is occupied by the first component. In the "west monsoon" (or rainy) season, on the contrary, the variances of the other components become comparably large to that of the first component. From the point of view of long-range forecasting of the rainfall in this area, this fact may be very important. That is, in the dry (and intermediate) seasons we should pay particular attention to the circulation patterns related to the QBO, while in the rainy season we should also note some other factors represented by the second and third components which may be inherent in this season. In other words, the above may be summarized as follows: the QBO mode in the Southern Hemisphere circulation may contribute effectively to the advance (or delay) of the beginning (or retreat) of the "west monsoon" season and the severely dry (or relatively wet) "east monsoon" season, but the rainfall amounts of the main "west monsoon" months also depend heavily on some other factors such as the influence of the Northern Hemisphere winter monsoon.

Table 3 Contributions of the First Four Components for Each Month of the Year

Component / Month	1	2	3	4	5-54
Jan.	17.8%	12.0	11.1	4.7	54.4
Feb.	14.2	10.2	4.4	3.7	67.5
Mar.	17.4	7.1	4.0	7.8	63.5
Apr.	22.5	3.0	5.0	2.2	67.3
May	47.6	1.2	5.0	2.7	43.5
Jun.	53.5	3.3	1.8	2.7	38.7
Jul.	55.8	3.4	1.0	2.6	37.2
Aug.	53.7	4.6	5.2	1.1	35.4
Sept.	28.0	3.8	6.8	3.3	58.1
Oct.	57.4	2.9	2.1	1.3	36.3
Nov.	31.6	6.9	5.5	8.6	47.4
Dec.	17.3	5.3	4.3	6.6	66.5

V Atmospheric Circulation Patterns Related to the Dominant Modes in the Anomaly Rainfall

V-1. The Quasi-biennial Oscillation (QBO) in the Southern Hemisphere

The first component of the anomaly rainfall over and around Java showed the QBO quite distinctly, with the maximum (or minimum) phases of the oscillation appearing frequently from June through August (refer to Fig. 6). The anomaly circulation patterns in the surface pressure field were then compared with the maximum and minimum rainfall of this component. In this analysis we utilized

the monthly mean surface pressure data[1)] for July given at 10° latitude-longitude intervals over the global region from 60°N to 50°S excluding the Atlantic Ocean area.

The mean composite maps for the years of the maximum rainfall (1956, 1957, 1958, 1959, 1962, 1968, and 1973) and of the minimum rainfall (1956, 1963, 1965, 1967, 1969, and 1972), and the map revealing the difference between the two are presented in Fig. 9. Fig. 9(c) shows a distinct pressure contrast between the areas over the eastern south Pacific and over and around Australia. The overall feature of the pattern over the Australia-New Zealand region rather resembles the P2 (the second component) pattern deduced by Trenberth [*ibid.*]. In addition, the variation of the time coefficients also correlates with that of the P2 pattern [*ibid.*] with the

1) This data provided by Prof. T. Chang of Beijing University, was originally compiled by Prof. S. Wong at Beijing University, Beijing, Peoples' Republic of China.

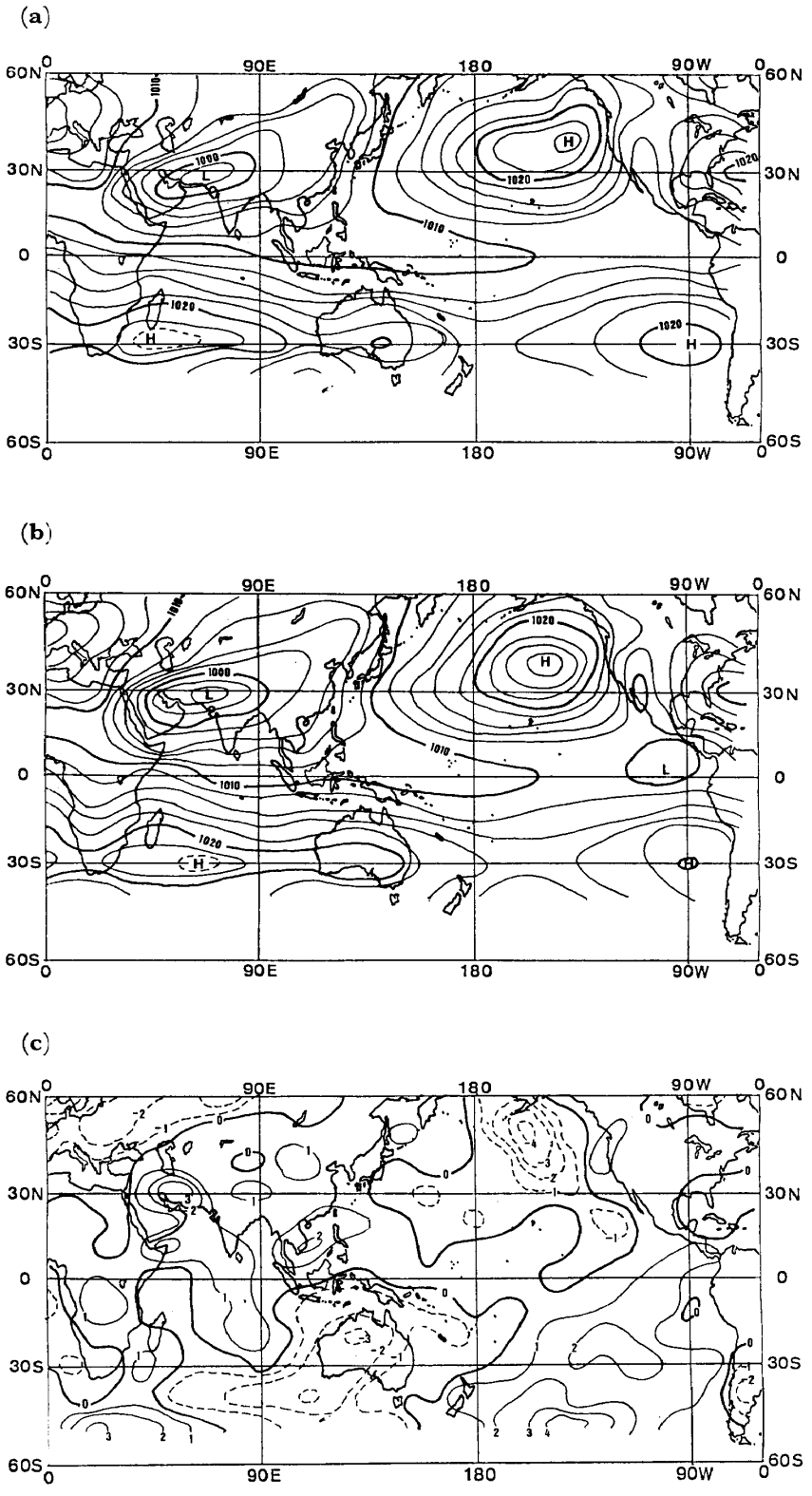

Fig. 9 Mean composite maps of the surface pressure in July for the years of (a) the maximum rainfall, (b) the minimum rainfall according to the first component, and (c) map of difference between the two ((a) minus (b)).

QBO mode. We may conclude, therefore, that the first component of the anomaly rainfall in Java undoubtedly corresponds with the QBO of the surface pressure field in the Southern Hemisphere. Trenberth [*ibid.*] supposed that the variation of this mode may have resulted from changes in amplitude and position of wavenumber 3 in the middle latitudes. The locations of the maximum (and minimum) anomalies in Fig. 9(c) suggests, however, wavenumber 2 is instead responsible for this mode. The synoptic situation for the maximum rainfall (Fig. 9(a)) shows that the southern Indian Ocean high is confined to the western half of the ocean near Madagascar island while the southern Pacific high is strong. That for the minimum rainfall (Fig. 9(b)) shows, in contrast, that the Indian Ocean high elongates eastward to the Australian continent while the Pacific high is relatively weak. Therefore, it seems that the eastward shift of the stationary wave (probably correspondent with wavenumber 2) from its normal position may cause the abnormally dry condition during the "east monsoon" season in and around Java. Associated with the change in the pressure pattern of the subtropical and mid-latitude zone from Fig. 9(a) to Fig. 9(b), the pressure field over the Indonesian region changes from a cyclonic to anticyclonic pattern, which may accompany the change in the divergence field. Moreover, coupling of the relatively strong (weak) Indian Ocean high and relatively weak (strong) high over the dry Australian continent in Fig. 9(a) (Fig. 9(b)) may create a favorable (unfavorable) condition for the moisture supply to the Indonesian region. It is also interesting to note that the two centers of action in the Northern Hemisphere (e.g., the northern Pacific high and the Azores high) seem to show significant intensity changes between the two patterns (as shown in Fig. 9(c)). This may imply that the QBO dominating the Southern Hemisphere and the equatorial zone is also linked with the Northern Hemisphere circulation. This problem will be discussed elsewhere.

V-2. The Fluctuation of the Winter Monsoon Circulation in the Northern Hemisphere

The second component of the anomaly rainfall represents one of the dominant modes in the rainy (or "west monsoon") season. Actually, the months of large negative (or positive) time coefficients correspond almost invariably with the above- (or below-) normal rainfall months for the whole island, usually January. In the same manner as described in the previous sub-section, the anomaly circulation patterns for January were prepared according to the years of large negative and positive time coefficients of this component. For the years of large negative coefficients (e.g., the maximum rainfall years for the Java Sea side), 1959, 1962, 1963, 1965, 1971, and 1972 were selected, and for the large positive coefficients (e.g., the minimum rainfall years for the Java Sea side) 1957, 1958, 1964, 1966, 1969,

1970, and 1973 were selected. The mean composite maps for the maximum and the minimum rainfall on the Java Sea side, the map showing the difference between the two are presented in Fig. 10.

In Fig. 10 (a) the Siberian high distinctly extends southward to south China compared to the case in Fig. 10 (b) (note, for example, the contour line of 1020 mb) though the location and intensity of the high is substantially the same in both cases. In the western north Pacific region a remarkably large pressure difference is prominent between the two cases as evident in Fig. 10 (c). Although the Aleutian low itself is weaker in Fig. 10 (a) than in Fig. 10 (b), a relatively low pressure area expands toward the lower latitudes. This feature may be attributed to the southward (or northward) shift of the cyclonic activity over the north Pacific in the case of Fig. 10(a) (Fig. 10 (b)). That is, the southward (or north-

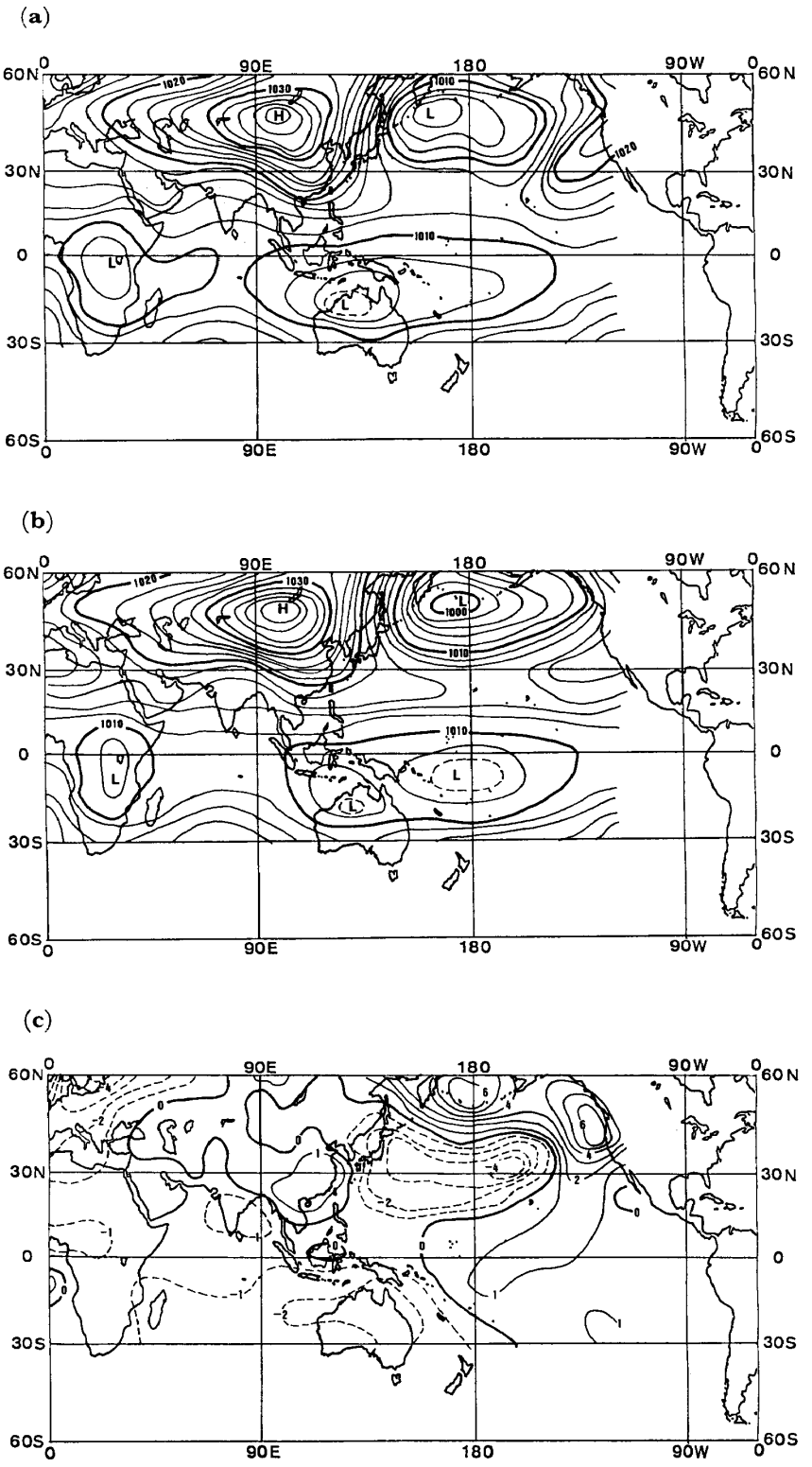

Fig. 10 Mean composite maps of the surface pressure in January for the years of (a) the maximum rainfall, (b) the minimum rainfall in the Java Sea side according to the second component, and (c) map of difference between the two ((a) minus (b)).

ward) shift of the winter monsoon circulation system over the Asiatic continent through the north Pacific may be responsible for the maximum (or minimum) rainfall in Java (especially on the Java Sea side). It should also be noted that in Fig. 10(a) the center of the equatorial through (low pressure) zone is located over northern Australia, whereas in Fig. 10(b) it is located over the western south Pacific with weaker intensity. This anomaly pattern of the Southern Hemisphere (Fig. 10(c)) reminds us of the "southern oscillation" pattern with the pressure contrast between the eastern Pacific and the Indian Ocean.

The anomaly patterns in Fig. 10 are nearly identical with those for the active (or weak) winter monsoon defined with reference to the strength of the easterly wind at 150 mb over Singapore by Tanaka [1980], since the selected typical years here are nearly the same as his. He commented that the anomaly circulation patterns including the Northern Hemisphere are closely connected with the southern oscillation with a periodicity of several years or more. White and Walker [1973] also found an association of the winter circulation over the north Pacific with the southern oscillation.

VI Summary and Remarks

Through the analysis of the long-term fluctuation of the monthly rainfall (1951–1973), we found that the variability of the rainfall in and around Java is large in the "east monsoon" (dry) season and relatively small in the "west monsoon" (rainy) season.

The EOF analysis of the anomaly rainfall from 1956 to 1973 revealed that the quasi-biennial oscillation (QBO) is dominant over the whole of Java with a large variance (29.4% of the total variance) and that the variability in the "east monsoon" season is mostly explained by this component. It was also confirmed that this mode in the anomaly rainfall is closely connected with the QBO in the surface pressure field over Australasia through the eastern south Pacific described by Trenberth [1975]. The second component (6.2% of the total variance) represents the variation in the "west monsoon" season with a contrastive spatial pattern between the Java Sea side and the Indian Ocean side of the island. This component seems to depend mostly upon the increase or decrease of the "west monsoon" rainfall on the Java Sea side with a larger amplitude than on the Indian Ocean side. This mode may be associated with the north- (or south-) ward shift of the winter monsoon circulation system in the Northern Hemisphere which may be linked with the southern oscillation in a time scale of several years or more.

In recent years not a few studies have attempted the problem of the preferred time scales and related spatial structures of the southern oscillation (e.g., Troup [1965], Kidson [1975], Trenberth [1976], etc.), though conclusive results have not been obtained yet. Through the present analysis, however, we can postulate that

there exist at least two modes of the southern oscillation in a broad sense with different time scales (of about two years and several years or more) which affect (or, may be affected by) the rainfall variation in the Indonesian "maritime continent." However, the problem still remains as to why these two modes have large seasonal dependencies in relation to the rainfall variation in this area. This problem may reveal some important clues for understanding the mechanism of the southern oscillation.

Acknowledgements

The rainfall data utilized in the present analysis was collected and compiled as part of the international project on "The Impact on Man of Climatic Change" organized by IFIAS (International Federation of Institutes for Advanced Studies). The author is indebted to Prof. S. Ichimura, Dr. H. Tsujii (Kyoto University) and Dr. S. Hasegawa (Osaka Prefectural University) for permitting him to use this data. He also thanks Dr. H. Furukawa for his helpful comments. The computation was made at the Data Processing Center of Kyoto University. This work was financially supported in part by Grant in Aid for Scientific Research from the Ministry of Education.

Appendix: The Empirical Orthogonal Function Analysis

Equation (1) can be written in vector form

$$\boldsymbol{P}_t=\boldsymbol{F}\boldsymbol{f}_t \qquad \text{(I-1)}$$

where

$$\boldsymbol{P}_t=\begin{bmatrix} P'(1,t) \\ P'(2,t) \\ \vdots \\ P'(m,t) \end{bmatrix}, \quad \boldsymbol{f}_t=\begin{bmatrix} f_1(t) \\ f_2(t) \\ \vdots \\ f_m(t) \end{bmatrix}$$

and

$$\boldsymbol{F}=\begin{bmatrix} F_1(1) & F_1(2) & \cdots & F_1(n) \\ F_2(1) & F_2(2) & \cdots & F_2(n) \\ \vdots & \vdots & \ddots & \vdots \\ F_m(1) & F_m(2) & \cdots & F_m(n) \end{bmatrix}$$

Then, the transposed matrix of (I-1) is multiplied by both sides of (I-1), and the ensemble mean of the product is made as follows:

$$E[\boldsymbol{P}\boldsymbol{P}^T]=\boldsymbol{F}E[\boldsymbol{f}\boldsymbol{f}^T]\boldsymbol{F}^T \qquad \text{(I-2)}$$

where $E[\ ]$ means the ensemble mean.

Here, the left-hand side of (I-2) is equal to the covariance matrix of $P'(i, t)$. In this case, as $P'(i, t)$ is normalized, it is equal to the correlation matrix of $P'(i, t)$:

$$\boldsymbol{R}=E[\boldsymbol{P}\boldsymbol{P}^T]$$

where $\boldsymbol{R}$ is the correlation matrix of $P'(i, t)$.

Under the condition of orthogonality as shown in (2), (I-2) can be rewritten as follows:

$$\boldsymbol{R}=\boldsymbol{F}\begin{bmatrix} \lambda_1 & & & 0 \\ & \lambda_2 & & \\ & & \ddots & \\ 0 & & & \lambda_m \end{bmatrix}\boldsymbol{F}^T \qquad \text{(I-3)}$$

If we add the condition that $\boldsymbol{F}$ is normalized as

$$\boldsymbol{F}\boldsymbol{F}^T=\boldsymbol{e}$$

where $\boldsymbol{e}$ is a unit vector, then, (I-3) is transformed as

$$\boldsymbol{R}\boldsymbol{F}=\boldsymbol{F}\begin{bmatrix} \lambda_1 & & & 0 \\ & \lambda_2 & & \\ & & \ddots & \\ 0 & & & \lambda_m \end{bmatrix}$$

or

$$\boldsymbol{R}\boldsymbol{F}_i=\lambda_i\boldsymbol{F}_i \qquad \text{(I-4)}$$

That is, (I-4) implies that λ_i corresponds with the i-th eigenvalue and $\boldsymbol{F}_i$ with the i-th component of the eigenvector of the correlation matrix $\boldsymbol{R}$. To obtain the eigenvalues and eigenvectors of $\boldsymbol{R}$, Jacobi's method was adopted in the computing procedure. Time coefficient vectors $\boldsymbol{f}_t$ were obtained by using $\boldsymbol{F}$ and $\boldsymbol{P}_t$ as follows:

$$\boldsymbol{f}_t=[\boldsymbol{F}^T\boldsymbol{F}]^{-1}\boldsymbol{F}^T\boldsymbol{P}_t=\boldsymbol{F}^T\boldsymbol{P}_t \qquad \text{(I-5)}$$

References

Berlage, H. P. 1961. Variations in the General Atmospheric and Hydrospheric Circulation of Periods of a Few Years Duration Affected by Variation of Solar Activity. *Annals New York Academy of Science* 95: 354–367.

Bjerknes, J. 1969. Atmospheric Teleconnections From the Equatorial Pacific. *Monthly Weather Review* 97(3): 163–172.

Blackman, R. B.; and Tukey, J. W. 1958. *The Measurement of Power Spectra.* New York: Dover Publications.

Kamimoto, Y. 1981. Monsuun Ajia ni Okeru Kakikousuiryo no Hendo [Variation of Summer Rainfall over Monsoon Asia]. Master Thesis, Faculty of Science, Kyoto University.

Kidson, John W. 1975. Tropical Eigenvector Analysis and the Southern Oscillation. *Monthly Weather Review* 103(3): 187–196.

Ramage, C. S. 1968. Role of a Tropical "Maritime Continent" in the Atmospheric Circulation. *Monthly Weather Review* 96(6): 365–369.

Tanaka, M. 1980. Role of the Circulation at the 150 mb Level in the Winter and Summer Monsoon in the Asian and Australian Regions. *Climatological Notes* 26: 1–134.

Trenberth, K. E. 1975. A Quasi-Biennial Standing Wave in the Southern Hemisphere and Interrelations with Sea Surface Temperature. *Quarterly Journal of the Royal Meteorological Society* 101: 55–74.

———. 1976. Spatial and Temporal Variations of the Southern Oscillation. *Quarterly Journal of the Royal Meteorological Society* 102: 639–653.

Troup, A. J. 1965. The 'Southern Oscillation.' *Quarterly Journal of the Royal Meteorological Society* 91: 490–506.

Walker, G. T. 1924. Correlation in Seasonal Variations of Weather, IX: A Further Study of World Weather. *Memoirs of the India Meteorological Department* 24(9): 275–332.

Walker, G. T.; and Bliss, E. W. 1932. World Weather V. *Memoir of the Royal Meteorological Society* 4(36): 53–84.

———. 1937. World Weather VI. *Memoir of the Royal Meteorological Society* 4(39): 119–139.

White, W. B.; and Walker, A. E. 1973. Meridional Atmospheric Teleconnections Over the North Pacific From 1950 to 1972. *Monthly Weather Review* 101(11): 817–822.

〔要　約〕

ジャワ島周辺における月降水量の時空間変動の解析

ジャワ島およびその周辺地域における23年間（1951–1973）の月降水量変動を解析した結果，変動度（variability）は，乾期（東風卓越期）に大きく，雨期（西風卓越期）には比較的小さいこと，地域的には，インド洋側がジャワ海側より大きいことが明らかとなった。

経年変動の時間的空間的特性を，平年偏差値についての経験的直交函数解析を用いて調べた。その結果，準2年周期振動（QBO）がもっとも卓越する成分（総分散の29.4%）として現われ，この振動は，ジャワ島のみならず，少なくともスマトラ，ボルネオ，スラウェシ各島の南半部にまで拡がる地域で，ほぼ同位相を持って卓越していることが明らかとなった。乾期における大きな変動度は，このQBOが大きく寄与しており，乾期(雨期)の伸縮，時期的なずれ，乾期降水量の増減を決める因子として重要なモードと推測される。第2成分（総分散の6.2%）は，雨期最盛期（1，2月）の降水量変動を説明しており，数年（以上）の長周期変動として現われている。空間パターンは，島の北側平野部と南側山岳部が逆の位相で変動していることを示している。

上記ふたつの卓越成分に関連した大気循環パターンを，グローバルな地上気圧資料を用いて調べた結果，第1成分は，オーストラリア周辺から南太平洋東部域を中心とする南半球中緯度の気圧のQBOに対応したものであり，第2成分は，北半球冬期のモンスーン循環系（シベリア高気圧—アリューシャン低気圧）の南北方向の偏位に関連していることが確認された。これらふたつの変動モードと，いわゆる"southern oscillation"との関連についても，若干の考察を試みた。